

Performance Analysis of Time Hopping and Direct Sequence UWB Space-Time Systems

W. Pam Siritwongpairat, Masoud Olfat, and K. J. Ray Liu

Department of Electrical and Computer Engineering,

University of Maryland, College Park, MD 20742, USA. {wipawee, molfat, kjrlui}@eng.umd.edu

Abstract—In this paper, we analyze the performance of Ultra-WideBand (UWB) Multiple-Input Multiple-Output (MIMO) systems employing various modulation and multiple access schemes, including Time Hopping (TH) Binary Pulse Position Modulation (BPPM), TH Binary Phase Shift Keying (BPSK), and Direct Sequence (DS) BPSK. We quantify the performance merits of UWB Space-Time (ST) systems regardless of the specific coding technique. We introduce a framework that enables us to compare UWB-MIMO systems with conventional UWB single-antenna systems in terms of diversity and coding gains. We show that the combination of ST coding and Rake architecture is capable of exploiting spatial diversity as well as multipath diversity, richly inherent in UWB environments. We find the upper bound on the average Pairwise Error Probability (PEP) under the hypothesis of quasi-static Nakagami- m frequency selective fading channels. Finally, simulation results are presented to support the theoretical analysis.

I. INTRODUCTION

Ultra-WideBand (UWB) technology is defined as a transmission scheme that occupies a bandwidth of more than 20% of its center frequency, or typically more than 500 MHz. The Multiple-Access (MA) capability of UWB system can be attained by incorporating the UWB signal with a pseudo-random Time Hopping (TH) or spreading sequence. With its unique properties of extensive multipath diversity and support for MA, UWB is a viable candidate for short range communications in dense multipath environments.

Multiple-Input Multiple-Output (MIMO) system has been well known for its potential of improving system performance under multipath scenarios. By the use of Space-Time (ST) coding techniques, MIMO can provide both diversity and coding advantages simultaneously, and hence yield high spectral efficiency and remarkable quality improvement.

To exploit the benefits of both UWB and MIMO systems, UWB ST coded scheme has been proposed [1]. The authors in [1] suggested an UWB ST coded system based on repetition code, which is a special case of what we present in this work. In this paper, we consider UWB ST systems with various modulation and MA schemes including TH Binary Pulse Position Modulation (BPPM) [2], TH Binary Phase Shift Keying (BPSK) [3], and Direct Sequence (DS) BPSK [4]. We quantify the performance figures of UWB ST systems regardless of specific coding scheme. Based on quasi-static Nakagami- m frequency selective fading channel model, we characterize the performances of UWB ST systems with the diversity and the coding gains. We utilize the Real Orthogonal Design (ROD) [5] as the engine code for UWB ST codes. Our simulation results show that DS-UWB-MIMO transmission provides superior performance in both single-user and multi-user scenarios.

The rest of the paper is organized as follows. Section II describes the models of UWB ST signals. The structure of UWB-MIMO receivers and the analysis of the received UWB ST signals are presented in Section III. In Section IV, we investigate the system performances in terms of the upper bound of the Pairwise Error Probability (PEP). The performances of UWB ROD ST codes are evaluated in Section V. Section VI describes numerical results and finally Section VII concludes the paper.

II. UWB ST SIGNAL MODELS

We consider UWB-MIMO multi-user environment with N_u users, each equipped with N_t transmit antennas, and a receiver with N_r receive antennas. At each transmitter, the input binary symbol sequence (coded or uncoded) is divided into blocks of N_b symbols. Each block is encoded into a ST codeword to be transmitted over N_t transmit antennas during K time slots. Since K time slots are required to transmit N_b symbols, the code rate is $R = N_b/K$. Each ST codeword matrix can then be expressed as an $K \times N_t$ matrix D_u whose $(k, i)^{th}$ element is $d_u^i(k)$, $d_u^i(k) \in \{-1, 1\}$, which represents the binary symbol transmitted by the u^{th} user at transmit antenna i over time slot k . The transmitter converts the ST codeword D_u into UWB ST signal matrix $\tilde{X}_u(t)$ whose $(k, i)^{th}$ element is the transmitted UWB signal $\tilde{x}_u^i(k; t)$ corresponding to the symbol $d_u^i(k)$. The signal $\tilde{x}_u^i(k; t)$ depends on the particular MA and modulation schemes and will be discussed in the following subsections.

A. TH-BPPM

The information of TH-BPPM system is conveyed by the positions of the pulses. The transmitted signal can be described as [2]

$$\tilde{x}_u^i(k; t) = \sqrt{\frac{E_u}{N_t}} \tilde{w} \left(t - kT_f - c_u(k)T_c - \frac{1 - d_u^i(k)}{2} T_d \right), \quad (1)$$

where $\tilde{w}(t)$ is the transmitted monocycle of duration T_w , and T_f is the pulse repetition period with $T_f \gg T_w$. The monocycle is normalized to have unit energy, and the factor $\sqrt{E_u/N_t}$ ensures that the total transmitted energy of the u^{th} user is E_u during each frame interval, independent of the number of transmit antennas. Each frame contains N_c subinterval of T_c seconds where $N_c T_c \leq T_f$. The TH sequence of the u^{th} user is denoted by $\{c_u(k)\}$, $0 \leq c_u(k) \leq N_c - 1$. It provides an additional time shift of $c_u(k)T_c$ seconds to the k^{th} monocycle in order to allow MA without catastrophic collisions. T_d represents the modulation delay which is used to distinguish between pulses carrying information $d_u^i(k) \in \{-1, 1\}$. Since an interval of $T_w + T_d$ second is used for one symbol modulation, the hop duration is chosen to satisfy $T_c = T_w + T_d$.

B. TH-BPSK

TH-BPSK scheme exploits the TH sequence concept as does in the TH-BPPM. However, the information in TH-BPSK system is carried in the polarities of the pulses. The transmitted UWB TH-BPSK signal is given by [3]

$$\tilde{x}_u^i(k; t) = \sqrt{\frac{E_u}{N_t}} d_u^i(k) \tilde{w}(t - kT_f - c_u(k)T_c). \quad (2)$$

Similar to the TH-BPPM case, each frame contains only one monocycle with a delay corresponding to the assigned TH sequence, $\{c_u(k)\}$, $0 \leq c_u(k) \leq N_c - 1$. Since the modulation interval is T_w , the hop duration is selected such that $T_c = T_w$. The monocycle is normalized to have unit energy, and the total transmitted energy per frame of the u^{th} user is E_u .

C. DS-BPSK

In DS-BPSK systems, the information is spread by a sequence of multiple monocycles whose polarities are determined by the spreading sequence $\{c_u(n_c)\}_{n_c=0}^{N_c-1}$, $c_u(n_c) \in \{-1, 1\}$. The transmitted DS-BPSK signal is modelled as [4]

$$\tilde{x}_u^i(t) = \sum_{k=0}^{K-1} \sqrt{\frac{E_u}{N_t N_c}} d_u^i(k) \sum_{n_c=0}^{N_c-1} c_u(n_c) \tilde{w}(t - kT_f - n_c T_c). \quad (3)$$

The frame interval T_f is divided into N_c segments of duration T_c . The hop period is chosen to satisfy $T_c = T_w$. Since each frame contains N_c normalized monocycles, we introduce the factor $\sqrt{1/N_c}$ to ensure that the sequence of N_c monocycles has unit energy. With the factor $\sqrt{E_u/N_t}$ being included, the transmitted energy per frame is E_u .

III. UWB-MIMO RECEIVER DESCRIPTIONS

We consider frequency selective channel model [6] where the channel of the u^{th} user is modelled as a tapped-delay line with L_u taps. The channels are assumed to be real, mutually independent and quasi-static, i.e., the channels remain constant over a block of K time slots. The channel impulse response from the i^{th} transmit antenna of the u^{th} user to the j^{th} receive antenna is given by

$$h_u^{ij}(t) = \sum_{l=0}^{L_u-1} \alpha_u^{ij}(l) \delta(t - \tau_u(l)), \quad (4)$$

where $\{\alpha_u^{ij}(l)\}$ are the multipath gain coefficients, $\{L_u\}$ denote the number of resolvable paths, and $\{\tau_u(l)\}$ represent the path delays relative to the delay of the desired user's first arrival path. Without loss of generality, we consider the first user as the desired user, and assume that $\tau_0(0) = 0$. We analyze an asynchronous MA system in which the relative propagation delays are random variables derived from the uniform distribution. In order to simplify the analysis, we assume that the minimum resolvable delay is equal to the pulse width, as in [4]. To avoid the Inter-Symbol Interference (ISI), we choose the signal parameters to satisfy $N_c T_c + \max_u \{\tau_u(L_u - 1)\} \leq T_f$. The channel fading is assumed to be Nakagami- m distributed with a Probability Density Function (PDF)

$$p_{|\alpha_u^{ij}(l)|}(x) = \frac{2}{\Gamma(m)} \left(\frac{m}{\Omega_u(l)} \right)^m x^{2m-1} \exp\left(-\frac{m}{\Omega_u(l)} x^2\right),$$

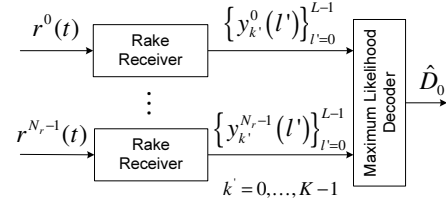


Fig. 1: UWB-MIMO receiver description.

where $\Gamma(\cdot)$ denotes the Gamma function, m is the fading parameter, and $\Omega_u(l)$ is the average power. We assume that $\{\tau_u(l)\}$ and $\Omega_u(l)$ of the l^{th} path are similar for every transmit-receive link. For the signal transmitted from the desired user, we assume that the TH or spreading sequence and Channel State Information (CSI) are known at the receiver.

At the receive antenna output, the shape of transmitted monocycle $\tilde{w}(t)$ is transformed to its second derivative due to the effect of propagation channel and the variation of antenna characteristics caused by large bandwidth [7]. Denote the received monocycle as $w(t)$ and define $x_u^i(k; t)$ similar to the transmitted waveform $\tilde{x}_u^i(k; t)$ by replacing $\tilde{w}(t)$ with $w(t)$. The received monocycle is assumed known at the receiver. The autocorrelation function of $w(t)$ is given by $\gamma(s) = \int_{-\infty}^{\infty} w(t-s)w(t)ds$, where $\gamma(0) = 1$. The received signal at receive antenna j comprises the signal from the desired user, MAI and noise, i.e., $r^j(t) = r_0^j(t) + n_{MU}^j(t) + n^j(t)$, where $n_{MU}^j(t) = \sum_{u=1}^{N_u-1} r_u^j(t)$,

$$r_u^j(t) = \sum_{i=0}^{N_t-1} \sum_{k=0}^{K-1} \sum_{l=0}^{L_u-1} \alpha_u^{ij}(l) x_u^i(k; t - \tau_u(l))$$

denotes the signal from user u , and $n^j(t)$ is real additive white Gaussian noise process with zero mean and two-sided power spectral density $N_0/2$.

At the receiver, we employ L -finger ($L \leq \max_u \{L_u\}$) Rake receivers, each adopting a reference waveform $v_{k'}(t)$ which comprises the delay versions of $w(t)$. The output of the l^{th} correlator at receive antenna j is given by

$$y_{k'}^j(l') = \int_{-\infty}^{\infty} v_{k'}(l') r^j(t) dt = y_{d,k'}^j(l') + n_{T,k'}^j(l'), \quad (5)$$

where $v_{k'}(l') \triangleq v_{k'}(t - \tau_0(l'))$, $y_{d,k'}^j(l')$ and $n_{T,k'}^j(l') \triangleq n_{MU,k'}^j(l') + n_{k'}^j(l')$ denote the correlator outputs corresponding to the desired transmitted data and the MAI plus thermal noise, respectively. Assuming no ISI, only the desired user's signal transmitted during the k^{th} frame will contribute to $y_{d,k'}^j(l')$. Thus, we can express $y_{d,k'}^j(l')$ as

$$y_{d,k'}^j(l') = \sum_{i=0}^{N_t-1} \sum_{l=0}^{L_0-1} \alpha_0^{ij}(l) \int_{-\infty}^{\infty} v_{k'}(l') x_0^i(k'; t - \tau_0(l)) dt. \quad (6)$$

The Rake receivers are followed by a Maximum Likelihood (ML) decoder where the decoding process is jointly performed across all N_r receive antennas, as shown in Fig. 1. In what follows, we analyze the receiver assuming different modulation and MA techniques employed.

A. TH-BPPM

The design of TH-BPPM receiver depends on the choice of the modulation delay, T_d . In the followings, $T_d = \arg \min_{T_d} \gamma(T_d)$,

as in [2]. The correlation waveform adopted at each Rake receiver is modelled as $v_{k'}(t) = w(t - k'T_f - c_0(k')T_c) - w(t - k'T_f - c_0(k')T_c - T_d)$. After some manipulations, we obtain

$$y_{k'}^j(l') = [1 - \gamma(T_d)] \sqrt{\frac{E_0}{N_t}} \sum_{i=0}^{N_t-1} d_0^i(k') \alpha_0^{ij}(l') + n_{T,k'}^j(l'),$$

which can be expressed in the matrix form as

$$\mathbf{Y}^j = [1 - \gamma(T_d)] \sqrt{E_0/N_t} D_0 \mathbf{A}_0^j + \mathbf{N}_T^j, \quad (7)$$

where D_0 is the desired user's transmitted ST symbol defined previously. Both matrices \mathbf{Y}^j and \mathbf{N}_T^j are of size $K \times L$ whose $(k, l)^{th}$ elements are $y_k^j(l)$ and $n_{T,k}^j(l)$, respectively. An $N_t \times L$ matrix \mathbf{A}_0^j represents the multipath gain coefficient matrix in which $(i, l)^{th}$ element is $\alpha_0^{ij}(l')$. Given the CSI on MIMO channels, the decoder performs ML decoding by selecting a codeword \hat{D}_0 which minimizes the square Euclidean distance between the hypothesized and actual correlator output matrices. The decision rule can be stated as

$$\hat{D}_0 = \arg \min_{D_0} \sum_{j=0}^{N_r-1} \|\mathbf{Y}^j - [1 - \gamma(T_d)] \sqrt{\frac{E_0}{N_t}} D_0 \mathbf{A}_0^j\|^2, \quad (8)$$

where $\|\mathbf{X}\|$ denotes the Frobenius norm of \mathbf{X} [8].

B. TH-BPSK

The reference waveform for TH-BPSK is $v_{k'}(t) = w(t - k'T_f - c_0(k')T_c)$. From (2) and (6), we find that $y_{d,k'}^j(l') = \sqrt{\frac{E_0}{N_t}} \sum_{i=0}^{N_t-1} d_0^i(k') \alpha_0^{ij}(l')$. Using (5), and rewriting all L correlator outputs of each receive antenna in the matrix form, we obtain

$$\mathbf{Y}^j = \sqrt{E_0/N_t} D_0 \mathbf{A}_0^j + \mathbf{N}_T^j, \quad (9)$$

in which \mathbf{Y}^j , \mathbf{A}_0^j and \mathbf{N}_T^j are in the same forms as the ones stated in (7). The decision rule can be written similar to (8) as

$$\hat{D}_0 = \arg \min_{D_0} \sum_{j=0}^{N_r-1} \|\mathbf{Y}^j - \sqrt{\frac{E_0}{N_t}} D_0 \mathbf{A}_0^j\|^2. \quad (10)$$

C. DS-BPSK

The DS-BPSK receiver adopts the monocycle sequence $v_{k'}(t) = \sqrt{1/N_c} \sum_{n_c=0}^{N_c-1} c_0(n_c) w(t - k'T_f - n_c T_c)$ as the reference waveform. Using (3) and (6), $y_{d,k'}^j(l')$ is given by

$$y_{d,k'}^j(l') = \sqrt{\frac{E_0}{N_t}} \sum_{i=0}^{N_t-1} d_0^i(k') \sum_{l=0}^{L_0-1} \alpha_0^{ij}(l) f(l, l'), \quad (11)$$

where $f(l, l') \triangleq N_c^{-1} \sum_{n_c=0}^{N_c-1} c_0(n_c) \sum_{n_c=0}^{N_c-1} c_0(n_c) \gamma((n_c - n_c')T_c + (\tau_0(l) - \tau_0(l')))$. Combining (11) and (5), the correlator output can be expressed in the matrix form as

$$\mathbf{Y}^j = \sqrt{E_0/N_t} D_0 \mathbf{A}_0^j \mathbf{F} + \mathbf{N}_T^j,$$

where \mathbf{F} is an $L_0 \times L$ matrix whose $(l, l')^{th}$ element is $f(l, l')$, and \mathbf{A}_0^j is of size $N_t \times L_0$ in which $(i, l)^{th}$ component is $\alpha_0^{ij}(l)$. Subsequently, the decision rule can be stated as

$$\hat{D}_0 = \arg \min_{D_0} \sum_{j=0}^{N_r-1} \|\mathbf{Y}^j - \sqrt{\frac{E_0}{N_t}} D_0 \mathbf{A}_0^j \mathbf{F}\|^2.$$

IV. PERFORMANCE ANALYSIS

First we can show that the noise sample $n_{k'}^j(l')$ is Gaussian distributed with zero mean and variance $\sigma_n^2 \triangleq \frac{N_0}{2} \int_{-\infty}^{\infty} v_{k'}^2(l') dt$. Define $n_{u,k'}^i(l, l') = \int_{-\infty}^{\infty} v_{k'}(l') x_u^i(t - \tau_u(l)) dt$. We express $n_{MU,k'}^j(l')$ (see (5)) as $n_{MU,k'}^j(l') = \sum_{u=1}^{N_u-1} \sum_{i=0}^{N_t-1} \sum_{l=0}^{L-1} \alpha_u^{ij}(l) n_{u,k'}^i(l, l')$. Using the same approach as in [7], one can show that $n_{u,k'}^i(l, l')$ is approximately Gaussian random variable with zero mean and variance $(E_u/N_t) \sigma_a^2$ where $\sigma_a^2 \triangleq \frac{1}{T_f} \int_{-\infty}^{\infty} \left[\int_{-\infty}^{\infty} w(t-s)v(t) dt \right]^2 ds$. Assuming independent Nakagami- m fading coefficients, independent of the transmitted signals, and using central limit theorem, we can show that for sufficiently large L , N_t and N_u , $n_{MU,m}^j(k)$ is approximately Gaussian random variable with zero mean and variance $\sigma_a^2 \sum_{u=1}^{N_u-1} E_u \sum_{l=0}^{L-1} \Omega_u(l)$. Hence, the MAI and noise $n_{tot,k'}^j(l')$ is zero mean Gaussian random variable with variance $\sigma_{n_T}^2 = \sigma_a^2 \sum_{u=1}^{N_u-1} E_u \sum_{l=0}^{L-1} \Omega_u(l) + \sigma_n^2$. Since the total noise and interference can be approximated with Gaussian distribution, PEP can be evaluated in a similar fashion as in the conventional narrowband MIMO system. The value of σ_n^2 , σ_a^2 , and PEP depend on particular modulation and MA techniques, and will be given in the following subsections.

A. TH-BPPM

Based on the reference signal in Section III-A, we can show that $\sigma_n^2 = [1 - \gamma(T_d)] N_0$, and $\sigma_a^2 = 2(\bar{\sigma}_a^2 - \sigma_d^2)$ where $\bar{\sigma}_a^2 \triangleq \frac{1}{T_f} \int_{-\infty}^{\infty} \gamma^2(s) ds$ and $\sigma_d^2 \triangleq \frac{1}{T_f} \int_{-\infty}^{\infty} \gamma(s) \gamma(s-T_d) ds$. Suppose that D_0 and \hat{D}_0 are two distinct transmitted ST codewords, following similar calculation steps as in [6], the PEP conditioned on the channel coefficient matrix $\{\mathbf{A}_0^j\}$ can be upper bounded by

$$P(D_0 \rightarrow \hat{D}_0 | \{\mathbf{A}_0^j\}) \leq \exp\left(\frac{-\rho}{4N_t} \sum_{j=0}^{N_r-1} \|(D_0 - \hat{D}_0) \mathbf{A}_0^j\|^2\right), \quad (12)$$

where $\rho = [1 - \gamma(T_d)]^2 E_0 / (2\sigma_{n_T}^2)$ which can be expressed as

$$\rho = \left[4 \frac{\bar{\sigma}_a^2 - \sigma_d^2}{[1 - \gamma(T_d)]^2} \sum_{u=1}^{N_u-1} \frac{E_u}{E_0} \sum_{l=0}^{L-1} \Omega_u(l) + \frac{2N_0/E_0}{[1 - \gamma(T_d)]} \right]^{-1}.$$

The upper bound of the PEP can be obtained by averaging (12) over all possible channel realizations. The resultant PEP can be found as [9]

$$P(D_0 \rightarrow \hat{D}_0) = \left[G_0(\tilde{m}) \frac{\rho}{4N_t} \right]^{-\tilde{m}rN_rL}, \quad (13)$$

where $G_0(\tilde{m}) \triangleq \tilde{m}^{-1} \left(\prod_{l=0}^{L-1} \Omega_0(l) \right)^{\frac{1}{L}} \left(\prod_{i=0}^{r-1} \lambda_i \right)^{\frac{1}{r}}$, $\tilde{m} = N_t m (N_t m - m + 1)^{-1}$, r is the rank and $\{\lambda_i\}_{i=0}^{r-1}$ represent nonzero eigenvalues of matrix $\mathbf{Z} \triangleq (D_0 - \hat{D}_0)^T (D_0 - \hat{D}_0)$. For a single user system, since there is no effect of MAI, ρ reduces to $[1 - \gamma(T_d)] E / 2N_0$. Thus, the PEP upper bound in (13) becomes

$$P(D_0 \rightarrow \hat{D}_0) \leq \left[G_0(\tilde{m}) \frac{[1 - \gamma(T_d)] E}{8N_t N_0} \right]^{-\tilde{m}rN_rL}.$$

In this case, the exponent $\tilde{m}rN_rL$ determines the slope of the performance curve plotted as a function of SNR, whereas the product $G_0(\tilde{m})$ displaces the curve. Hence, the minimum values of $\tilde{m}rN_rL$ and $G_0(\tilde{m})$ over all pairs of distinct codewords define the diversity gain and the coding gain, respectively.

B. TH-BPSK

Since the reference signal for TH-BPSK system is the shifted monocycle whose energy is unity, we can see that $\sigma_n^2 = N_0/2$ and $\sigma_a^2 = \bar{\sigma}_a^2$. Following the same calculations as for BPPM, the upper bound of the PEP can be expressed similar to (13) with identical $G_0(\tilde{m})$ and

$$\rho = \frac{E_0}{2\sigma_{n_{tot}}^2} = \left[2\bar{\sigma}_a^2 \sum_{u=1}^{N_u-1} \frac{E_u}{E_0} \sum_{l=0}^{L-1} \Omega_u(l) + \left(\frac{E_0}{N_0} \right)^{-1} \right]^{-1}, \quad (14)$$

which becomes E/N_0 for the single user system.

C. DS-BPSK

Using similar calculation steps as above, we obtain $\sigma_n^2 = N_0/2$ and $\sigma_a^2 = \bar{\sigma}_a^2$. The upper bound of the PEP conditioned on the channel matrix is given by $P(D_0 \rightarrow \hat{D}_0 | \{\mathbf{A}_0^j\}) \leq \exp\left(-\frac{\rho}{4N_t} \sum_{j=0}^{N_r-1} \beta^j\right)$ where $\beta^j \triangleq \|(D_0 - \hat{D}_0)\mathbf{A}_0^j\mathbf{F}\|^2$, and $\rho = E_0/(2\sigma_{n_{tot}}^2)$, which is in the same form as (14). Since \mathbf{Z} is a real symmetric matrix, it can be decomposed into $\mathbf{Z} = \mathbf{V}\mathbf{\Lambda}\mathbf{V}^T$, where $\mathbf{\Lambda}$ is a diagonal matrix whose diagonal elements are the eigenvalue of \mathbf{Z} . It follows that $\beta^j = \text{tr}\left(\mathbf{F}^T(\mathbf{A}_0^j)^T\mathbf{Z}\mathbf{A}_0^j\mathbf{F}\right) = \text{tr}\left((\mathbf{B}_0^j)^T\mathbf{\Lambda}\mathbf{B}_0^j\right)$, where $\text{tr}(\mathbf{X})$ stands for the trace of \mathbf{X} , and $\mathbf{B}_0^j \triangleq \mathbf{V}^T\mathbf{A}_0^j\mathbf{F}$. Let \mathbf{I}_x denote an $x \times x$ identity matrix, \otimes represent the tensor product, and $\mathbf{v}(\mathbf{X})$ stack the column of \mathbf{X} in a column vector. Then, we have

$$\sum_{j=0}^{N_r-1} \beta^j = \sum_{j=0}^{N_r-1} \text{tr}\left((\mathbf{B}_0^j)^T\mathbf{\Lambda}\mathbf{B}_0^j\right) = \mathbf{b}^T\Delta\mathbf{b},$$

where $\Delta \triangleq \mathbf{I}_{N_r L} \otimes \mathbf{\Lambda}$, and $\mathbf{b} \triangleq \left[\mathbf{v}^T(\mathbf{B}_0^0) \dots \mathbf{v}^T(\mathbf{B}_0^{N_r-1})\right]^T$. Denote the correlation matrix of \mathbf{b} by $\mathbf{R} = \mathbb{E}[\mathbf{b}\mathbf{b}^T]$. Since \mathbf{R} is nonnegative definite, it has a symmetric square root \mathbf{U} such that $\mathbf{R} = \mathbf{U}^T\mathbf{U}$ [8]. Let $\mathbf{q} = (\mathbf{U}^T)^{-1}\mathbf{b}$. Since $\mathbb{E}[\mathbf{q}\mathbf{q}^T] = \mathbf{I}_{N_t N_r L}$, the components of \mathbf{q} are uncorrelated. Now the conditioned PEP upper bound can be re-expressed as

$$P(D_0 \rightarrow \hat{D}_0 | \{\mathbf{A}_0^j\}) \leq \exp\left(-\frac{\rho}{4N_t}\mathbf{q}^T\mathbf{U}\Delta\mathbf{U}^T\mathbf{q}\right).$$

Assuming that \mathbf{R} is full rank, \mathbf{U} is also full rank [8]. Therefore, maximum diversity gain can be achieved by maximizing the rank of Δ , which is equivalent to $N_r L$ times the rank of \mathbf{Z} . Hence, the rank criterion for DS-UWB ST system is identical to that of TH-UWB ST system. In order to quantify the coding gain, it might be necessary to evaluate the statistics of \mathbf{q} which is difficult to obtain for Nakagami fading distribution. In Section VI, we perform simulations to further investigate the performance of DS-UWB ST system.

V. UWB ST CODES USING ROD

In this section, we consider 2 transmit antenna system employing ROD ST coding scheme [5]. Generalization to UWB ST systems with higher number of transmit antennas is straightforward. The user subscript u is omitted for notation simplicity. Exploiting full rate ROD code, the 2×2 matrix D is given by

$$D = \begin{pmatrix} d^0 & d^1 \\ -d^1 & d^0 \end{pmatrix}.$$

We can see that $\mathbf{Z} = 4\sum_{i=0}^1 \delta(d^i - \hat{d}^i)\mathbf{I}_2$. Define $S = [\mathbf{s}_1 \ \mathbf{s}_2]$, where $\mathbf{s}_1 = [1 \ -1]^T$ and $\mathbf{s}_2 = [1 \ 1]^T$. For ROD ST code with rate $1/K$ where K is an even integer, the ST codeword is given by $D = d(S^T \dots S^T)_{K \times 2}^T$, and $\mathbf{Z} = 4K\delta(d - \hat{d})\mathbf{I}_2$. Observe that both full and reduced rate codes result in two equal eigenvalues $\lambda_0 = \lambda_1 \triangleq \lambda$ and the codeword matrix difference $\lambda\mathbf{I}_2$ of full rank ($r = 2$). Substituting the eigenvalues into (13), we obtain

$$P(D \rightarrow \hat{D}) \leq \left[\prod_{l=0}^{L-1} \left(\frac{\Omega(l)\rho\lambda}{\tilde{m}} \frac{\rho\lambda}{8} \right) \right]^{-2\tilde{m}N_r}. \quad (15)$$

With \tilde{m} , $\{\Omega(l)\}$, L , and N_r being fixed, (15) depends only on the value of $\rho\lambda$. The higher the $\rho\lambda$, the better the performance.

Let us assume that the energy per bit E_b is fixed. For simplicity, we also assume that all users have equal transmitted energy per frame (E). Expressing E in term of E_b , we have $E = E_b$ for full rate and $E = E_b/K$ for $1/K$ rate codes. It is obvious that assuming one erroneous symbol, the eigenvalues for $1/K$ rate are K times larger than those for full rate code. We denote the eigenvalue of full rate code as $\bar{\lambda}$.

Consider the single user case. We observe that $\rho\lambda$ is equal to $[1 - \gamma(T_d)](E_b/2N_0)\bar{\lambda}$ for BPPM and $(E_b/N_0)\bar{\lambda}$ for BPSK, regardless of the code rate. As a result, reducing the code rate does not improve the performance of single user systems. In addition, $\rho\lambda$ of TH/DS-BPSK systems are $2[1 - \gamma(T_d)]^{-1}$ times that of TH-BPPM system. Since $[1 - \gamma(T_d)] < 2$, TH/DS-BPSK tend to outperform TH-BPPM system for every code rate. On the other hand, we show in [9] that the multi-user system with reduced rate provides higher value of $\rho\lambda$, and hence likely to performs better than that with full rate.

VI. SIMULATION RESULTS

We performed simulations for UWB MA systems based on TH-BPPM, TH-BPSK and DS-BPSK schemes. We employ UWB signals with $T_f = 100$ ns and T_w of 0.8 ns. The received monocycle is modelled as the second derivative of the Gaussian pulse [7]. The transmitted data takes value from $\{-1, 1\}$ with equal probability. The modulation delay for BPPM signal is $T_d = 0.22T_w$. The hop interval is $T_c = T_w + T_d$ for TH-BPPM and $T_c = T_w$ for TH/DS-BPSK systems. We adopt discrete uniform random TH and spreading sequence so as to evaluate the performances regardless of the choice of any particular code.

We consider quasi-static frequency selective fading channels in which the delay profile is generated according to [10]. The channel envelopes are Nakagami- m distributed with $m = 2$ and the power of L_u paths being normalized such that $\sum_{l=0}^{L_u-1} \Omega_u(l) = 1$. We assume that the power delay profiles of all users are similar. The thermal noise is real Gaussian random process with zero mean and variance $N_0/2$. The number of fingers for the Rake receiver is chosen to be $L = 4$.

Figs. 2 and 3 show the BER performance of TH and DS UWB systems in single-user and multi-user environments. We can see from both figures that MIMO systems outperform SISO systems, regardless of the modulation and MA techniques. Consider the single user case illustrated in Fig. 2. At any fixed SNR, the performances of TH-BPSK and DS-BPSK systems are close to each other, and both BPSK systems yield superior performances to TH-BPPM. This observation is consistent with the theoretical

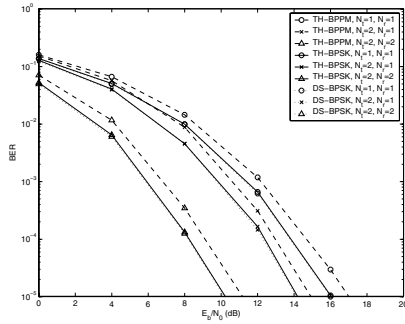


Fig. 2: TH and DS UWB single user systems.

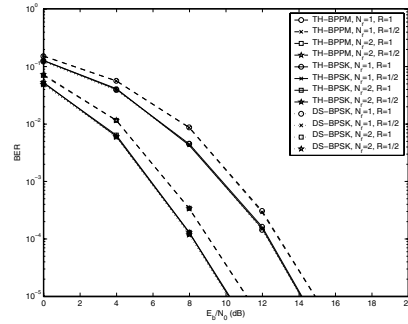


Fig. 4: UWB single user systems with ROD ST codes of different rates.

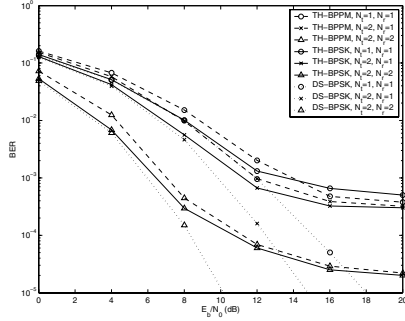


Fig. 3: TH and DS UWB multi-user ($N_u = 5$) systems.

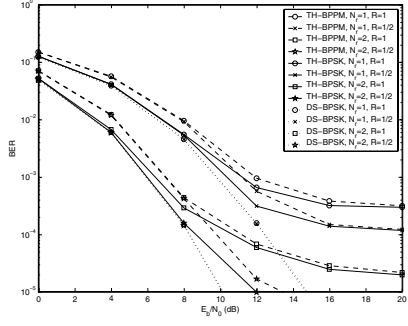


Fig. 5: UWB multi-user systems with ROD ST codes of different rates.

results given in Section V. In Fig. 3, we show the system performances when 5 asynchronous users are active. In low SNR regime, TH/DS-BPSK outperform TH-BPPM scheme, and both BPSK systems yield close performances. However, due to the MAI, the BER of TH multi-user systems slightly drop with increasing E_b/N_0 , and a high error floor can be noticed at high SNR. On the other hand, even in MA scenarios, we can still see considerable improvement of DS-BPSK ST system.

In Figs. 4 and 5, we show the performance of single and multiple user systems employing ROD ST codes with full and half rates. Both figures illustrate that BPSK provides lower BER than BPPM scheme, regardless of the code rate. From Fig. 4, we can see that the performances of full and half rate ROD codes are close to each other for every modulation schemes. This is in agreement with the results in Section V, which say that for single user system, decreasing the rate of ROD ST code does not improve the performance. Unlike the single user case, the results in Fig. 5 confirm our expectation that when the code rate is lower, both TH-BPSK and TH-BPPM multi-user systems achieve better performances, especially in high SNR regime. However, for DS-BPSK MA systems, the BER improvement obtained from reducing the code rate is insignificant. This is because for $N_u = 5$, the effect of MAI to DS system is considerably small, and ROD ST code provides close to maximum achievable performance without decreasing the code rate. Again, DS-BPSK ST system outperforms other modulation schemes.

VII. CONCLUSIONS

In this paper, we investigate the UWB ST systems utilizing TH-BPPM, TH-BPSK, and DS-BPSK signals. The performance metrics (diversity and coding gains) of UWB ST systems are quantified regardless of the particular coding scheme. We considered an example of UWB ST signals based on ROD ST code

for two transmit antenna system. Both analytical and simulation results show the performance improvement of the UWB MIMO systems over the conventional SISO systems. For example, by employing two transmit and one receive antennas for a system of 5 users and $E_b/N_0 = 8$ dB, the BER for TH-BPPM decreases from 1.5×10^{-2} to 9.7×10^{-3} , for TH-BPSK from 10^{-2} to 5.6×10^{-3} , and for DS-BPSK from 10^{-2} to 4.6×10^{-3} . We illustrate that in single user case, both DS-BPSK and TH-BPSK yields similar performance which is superior to TH-BPPM system, whereas in MA scenarios, DS-BPSK ST modulation outperforms other considered schemes.

REFERENCES

- [1] L. Yang and G. B. Giannakis, "Space-Time Coding for Impulse Radio", *IEEE Conf. on Ultra Wideband Systems and Tech.*, pp. 235-240, May 2002.
- [2] R. A. Scholtz "Multiple Access with Time-Hopping Impulse Modulation", *Proc. of MILCOM Conf.*, Boston, MA, USA, pp. 447 - 450, Oct. 1993.
- [3] M. L. Welborn, "System Considerations for Ultra-Wideband Wireless Networks", *IEEE Radio and Wireless Conf.*, pp. 5-8, Aug. 2001.
- [4] J. R. Foerster, "The Performance of a Direct-Sequence Spread UltraWideband System in the Presence of Multipath, Narrowband Interference, and Multiuser Interference", *IEEE Conf. on Ultra Wideband Systems and Tech.*, pp. 87-91, May 2002.
- [5] V. Tarokh, H. Jafarkhani and A. R. Calderbank, "Space-Time Block Codes from Orthogonal Designs", *IEEE Trans. on Inform. Theory*, vol. 45, no. 5, pp. 1456-1467, Jul. 1999.
- [6] J. G. Proakis, *Digital Communications*, McGraw-Hill, New York, 2001.
- [7] M. Z. Win and R. A. Scholtz, "Ultra-Wide Bandwidth Time-Hopping Spread-Spectrum Impulse Radio for Wireless Multiple-Access Communications", *IEEE Trans. on Commun.*, vol. 48, no. 4, pp. 679-691, Apr. 2000.
- [8] R. A. Horn and C. R. Johnson, *Matrix Analysis*, Cambridge Univ. Press, New York, 1985.
- [9] W. P. Siritwongpairat, M. Olfat, and K. J. R. Liu, "Performance Analysis and Comparison of Time Hopping and Direct Sequence UWB-MIMO Systems", *EURASIP J. on Applied Signal Proc. Special Issue on "UWB-State of the Art"*, to appear.
- [10] S. S. Ghassemzadeh, L. J. Greenstein, T. Sveinsson, and V. Tarokh, "A Multipath Intensity Profile Model for Residential Environments", *IEEE Wireless Commu. and Networking Conf.*, vol. 1, pp. 150 - 155, Mar. 2003.